Impact on metal coordination and pH on the antimicrobial activity of histatin 5 and the products of its hydrolysis

Emilia Dzień,[a] Joanna Wątły,*[a] Arian Kola,[b] Aleksandra Mikołajczyk,[c] Adriana Miller,[a] Agnieszka Matera-Witkiewicz,[c] Daniela Valensin[b] and Magdalena Rowińska-Żyrek*[a]

[a] Faculty of Chemistry, University of Wrocław, F. Joliot-Curie 14, 50-383 Wrocław, Poland
[b] Department of Biotechnology, Chemistry and Pharmacy, University of Siena, Via A. Moro 2, 53100 Siena, Italy
[c] Screening of Biological Activity Assays and Collection of Biological Material Laboratory, Wroclaw Medical University Biobank, Faculty of Pharmacy, Wroclaw Medical University, Borowska 211A, 50-556 Wrocław, Poland

Table S1. Potentiometric data for proton, Zn(II) and Cu(II) complexes with histatin 5, histatin 5-8 and histatin 8 at T = 298 K and I = 0.1 M $NaClO_4$. The standard deviations are reported in parentheses as uncertainties on the last significant figure.

	Histatin 5 (DSHAKRHHGYKRKFHEKHHSHRGY)		Histatin 5-8 (DSHAKRHHGYKR)		Histatin 8 (KFHEKHHSHRGY)	
species	logβ[a]	pKa[b]	logβ[a]	pKa[b]	logβ[a]	pKa[b]
$H_{16}L$	121.11(1)	2.63(D)				
$H_{15}L$	118.48(1)	3.64(E)				
$H_{14}L$	114.84(1)	5.14(H)				
$H_{13}L$	109.70(1)	5.60(H)				
$H_{12}L$	104.10(2)	5.98(H)				
$H_{11}L$	98.12(2)	6.16(H)				
$H_{10}L$	91.96(2)	6.67(H)				
H_9L	85.29(1)	6.81(H)			70.16(1)	3.53(E)
H_8L	78.48(1)	7.72(H)	62.98(2)	2.79(D)	66.63(1)	5.47(H)
H_7L	70.76(1)	9.24(NH_2)	60.19(2)	5.56(H)	61.16(1)	6.13(H)
H_6L	61.52(2)	9.38(Y)	54.63(1)	6.34(H)	55.03(1)	6.60(H)
H_5L	52.14(1)	9.91(Y)	48.29(2)	7.27(H)	48.43(1)	7.37(H)
H_4L	42.23(3)	10.21(K)	41.02(1)	9.42(NH_2)	41.06(1)	9.43(NH_2)
H_3L	32.02(1)	10.22(K)	31.60(2)	9.81(Y)	31.63(1)	9.88(Y)
H_2L	21.80(2)	-	21.79(1)	10.77(K)	21.75(1)	10.68(K)
HL		-	11.02(2)	11.02(K)	11.07(1)	11.07(K)
Cu(II) complexes						
$CuH_{11}L$	105.64(1)	-	-	-	-	-
$CuH_{10}L$	100.62(3)	5.02	-	-	-	-
CuH_9L	94.86(7)	5.76	-	-	-	-
CuH_8L	89.06(5)	5.80	-	-	-	-
CuH_7L	82.63(7)	6.43	-	-	-	-
CuH_6L	76.07(4)	6.56	-	-	-	-
CuH_5L	68.86(3)	7.21	-	-	57.66(2)	-
CuH_4L	59.77(6)	9.09	50.76(1)	-	52.89(3)	4.77
CuH_3L	50.22(6)	9.55	44.85(3)	5.91	46.81(5)	6.08
CuH_2L	40.26(9)	9.96	38.39(3)	6.46	39.79(6)	7.02
CuHL	30.02(8)	10.24	28.94(5)	9.45	29.87(8)	9.92

CuL	19.65(5)	10.37	19.09(3)	9.85	19.83(6)	10.04
$CuH_{-1}L$	-	-	-	-	-	-
$CuH_{-2}L$	-2.25(4)	-	-2.34(4)	-	-2.82(7)	-
Zn(II) complexes						
$ZnH_{10}L$	97.94(1)	-	-	-	-	-
ZnH_9L	-	-	-	-	-	-
ZnH_8L	86.27(1)	-	-	-	-	-
ZnH_7L	79.62(1)	6.65	-	-	-	-
ZnH_6L	71.84(1)	7.78	-	-	-	-
ZnH_5L	63.29(1)	8.55	-	-	52.90(1)	-
ZnH_4L			45.30(1)	-	46.52 (1)	6.38
ZnH_3L			38.06(1)	7.24	39.19(1)	7.33
ZnH_2L			30.15(1)	7.91	30.53(2)	8.65
ZnHL			21.21(2)	8.94		

[a] $\beta(H_jL_k) = [H_jL_k]/([H]^j[L]^k)$, in which [L] is the concentration of the fully deprotonated peptide.

[b] $\log\beta(H_jL_k) - \log\beta(H_{j-1}L_k) = pK_a$

In the Cu(II)-histatin 5 mass spectra (Fig. S1A), the prevailing signals correspond to the free ligand (*m/z* = 434.51, *z* = 7+; *m/z* = 506.76, *z* = 6+; *m/z* = 607.91, *z* = 5+ and *m/z* = 759.64, *z* = 4+). Signals which correspond to copper complex are also visible (*m/z* = 443.48, *z* = 7+; *m/z* = 517.23, *z* = 6+; *m/z* = 620.46, *z* = 5+ and *m/z* = 775.32, *z* = 4+).

In the Zn(II)-histatin 5 mass spectra (Fig. S1B), aside from the signals with come from the free ligand (*m/z* = 506.92, *z* = 6+ ; *m/z* = 608.10, *z* = 5+ ; *m/z* = 759.87, *z* = 4+) a zinc complexes (*m/z* = 517.40, *z* = 6+ ; *m/z* = 620.68, *z* = 5+ ; *m/z* = 775.35, *z* = 4) are visible.

In the Cu(II)-histatin 5-8 mass spectra (Fig. S1C), signals which come from the free ligand (*m/z* = 497.91, *z* = 3+ and *m/z* = 746.39, *z* = 2+) and a copper complexes (*m/z* = 518.23, *z* = 3+ and *m/z* = 776.84, *z* = 2+) are visible.
In the Zn(II)-histatin 5-8 mass spectra (Fig. S1D), beside from the signals which come from the free ligand (*m/z* = 497.93, *z* = 3+ and *m/z* = 746.39, *z* = 2+) signals from zinc complex (*m/z* = 523.30, *z* = 3+ and *m/z* = 777.34, *z* = 2+) are visible.

In the case of Cu(II)-histatin 8 mass spectra (Fig. S1E), the visible signals correspond to the free ligand (*m/z* = 521.58, *z* = 3+ and *m/z* = 756.31, *z* = 2+) and copper complex (*m/z* = 541.88, *z* = 3+ and *m/z* = 812.30, *z* = 2+).

In the Zn(II)-histatin 8 spectra (Fig. S1F), aside from the signals with come from the free ligand (*m/z* = 521.59, *z* = 3+ and *m/z* = 781.89, *z* = 2+), a zinc complex (*m/z* = 542.23, *z* = 3+ and *m/z* = 812.85, *z* = 2) and its adduct with two water molecules (*m/z* = 831.86, *z* = 2+) can be observed.

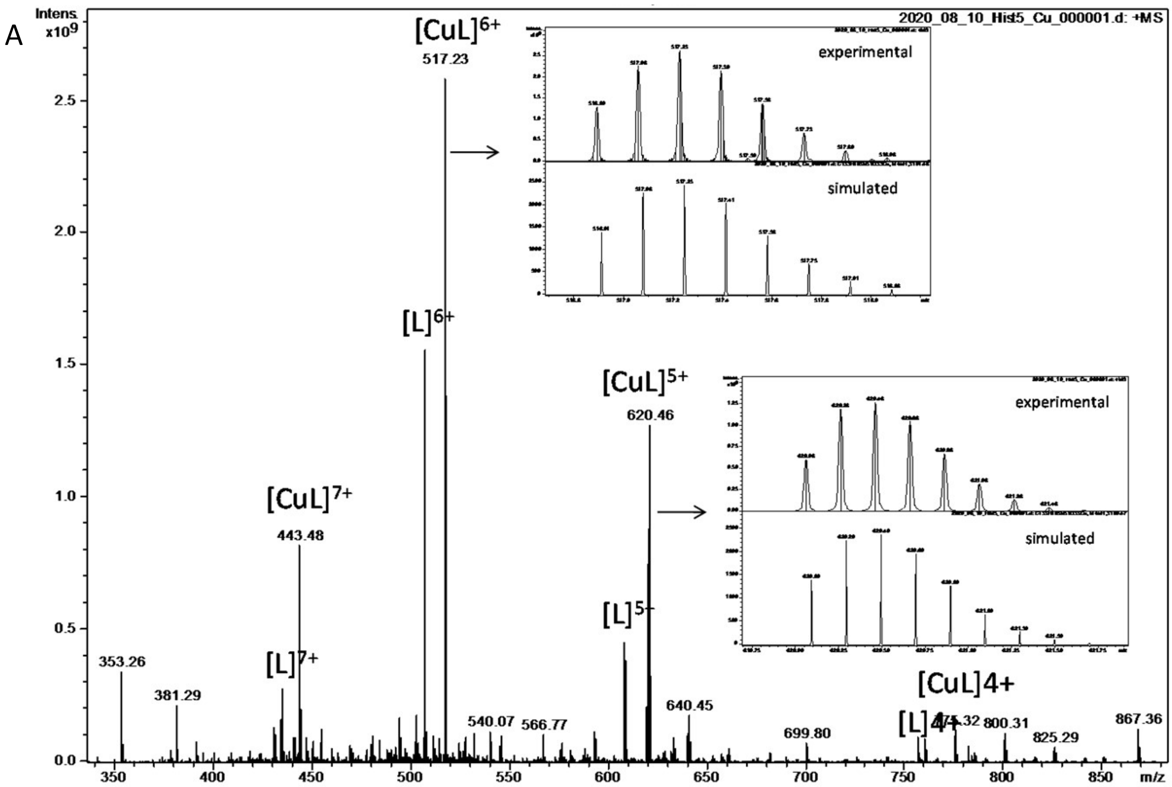
A
Intens. x10^9
2020_08_10_Hist5_Cu_000001.d: +MS
[CuL]^6+
517.23
experimental
simulated
[L]^6+
[CuL]^5+
620.46
[CuL]^7+
443.48
[L]^5+
[L]^7+
353.26
381.29
540.07
566.77
640.45
699.80
[CuL]4+
[L]4+
775.32
800.31
825.29
867.36
m/z

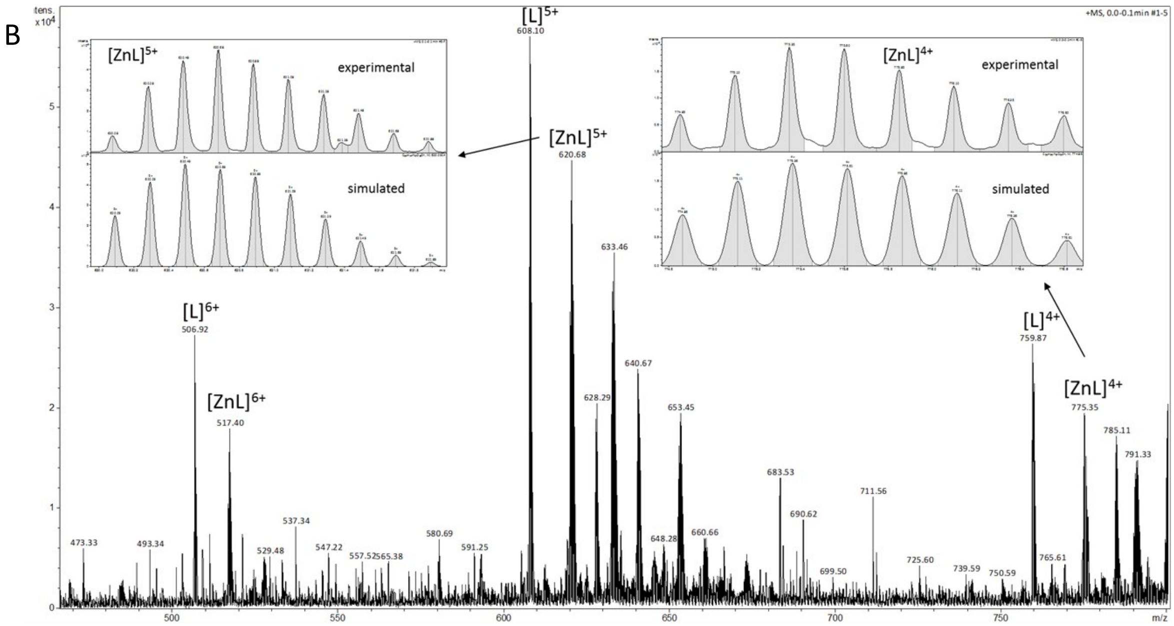
B
Intens. x10^4
+MS, 0.0-0.1min #1-5
[ZnL]^5+
experimental
simulated
[L]^5+
608.10
[ZnL]^5+
620.68
[ZnL]^4+
633.46
628.29
640.67
653.45
[L]^6+
506.92
[ZnL]^6+
517.40
[L]^4+
759.87
[ZnL]^4+
775.35
785.11
791.33
473.33
493.34
529.48
537.34
547.22
557.52
565.38
580.69
591.25
648.28
660.66
683.53
690.62
699.50
711.56
725.60
739.59
750.59
765.61
m/z

C

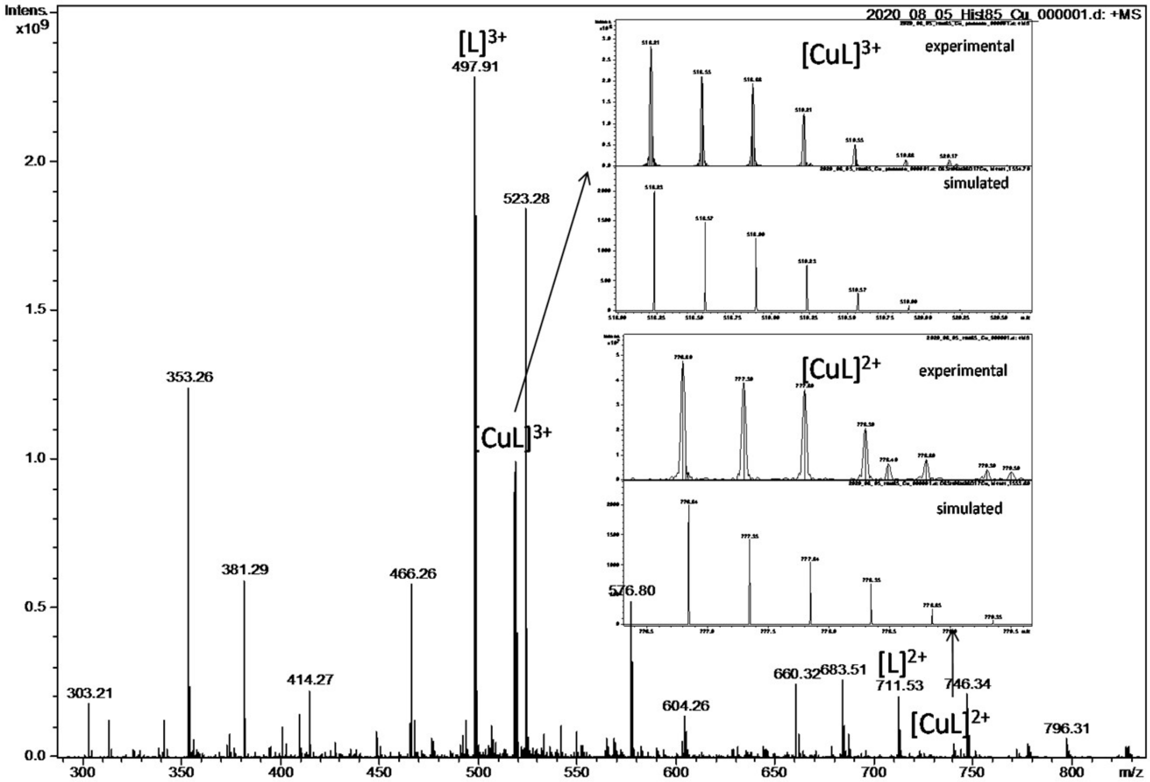

Intens.
x10^9
2020_08_05_Hist85_Cu_000001.d: +MS
[L]3+
497.91
[CuL]3+
experimental
simulated
523.28
[CuL]3+
[CuL]2+
experimental
simulated
353.26
381.29
466.26
576.80
414.27
303.21
604.26
660.32
683.51
[L]2+
711.53
746.34
[CuL]2+
796.31
m/z

D

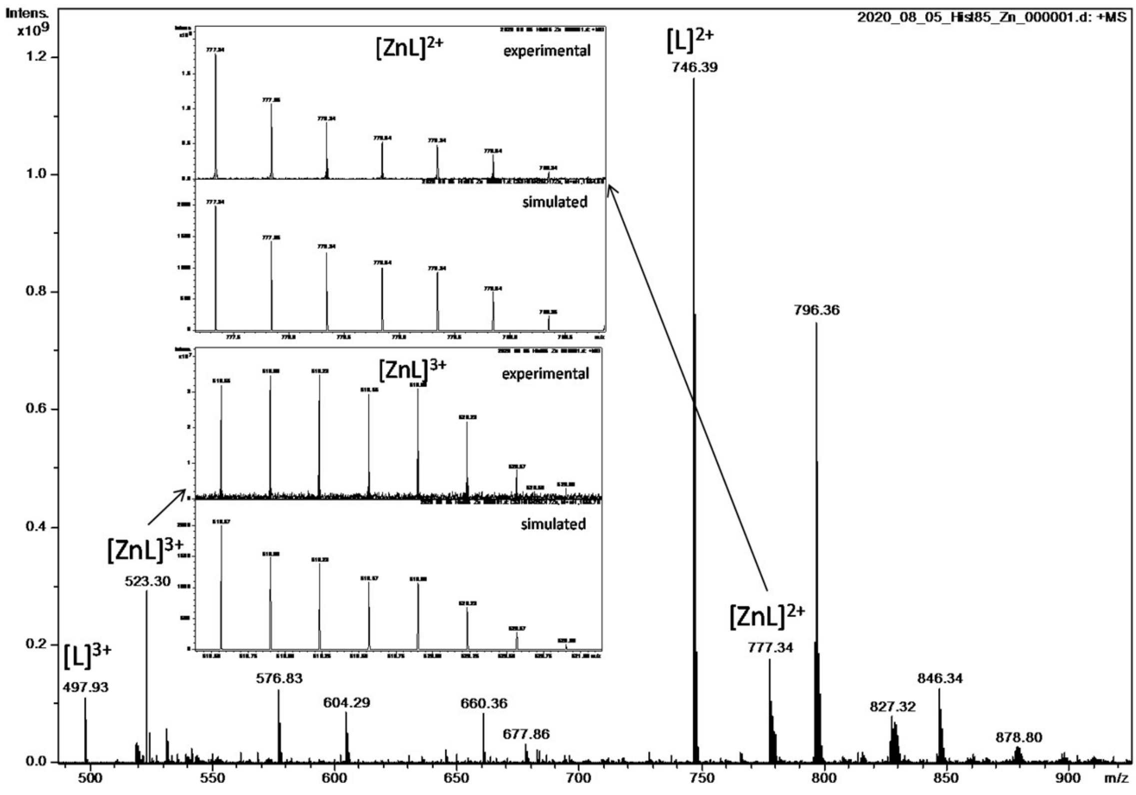

Intens.
x10^9
2020_08_05_Hist85_Zn_000001.d: +MS
[ZnL]2+
experimental
simulated
[ZnL]3+
experimental
simulated
[L]2+
746.39
796.36
[ZnL]3+
523.30
[ZnL]2+
777.34
[L]3+
497.93
576.83
604.29
660.36
677.86
827.32
846.34
878.80
m/z

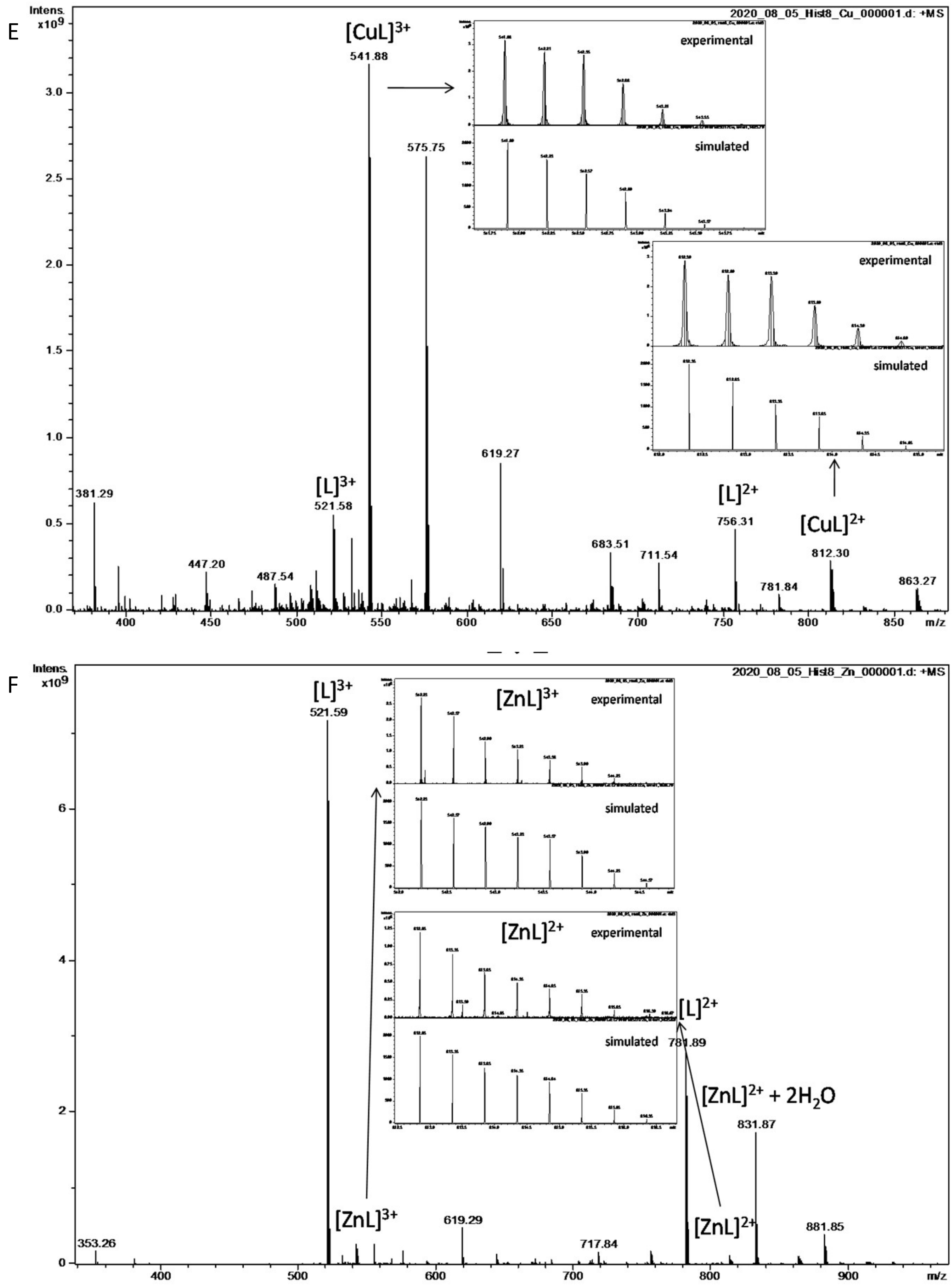

Fig. S1. ESI-MS spectra of: A) Cu(II)-histatin 3; B) Zn(II)-histatin 3; C) Cu(II)-histatin 3-4; D) Zn(II)-histatin 3-4; E) Cu(II)-histatin 4; F) Zn(II)-histatin 4; M:L molar ratio = 1:1, pH = 7.4.

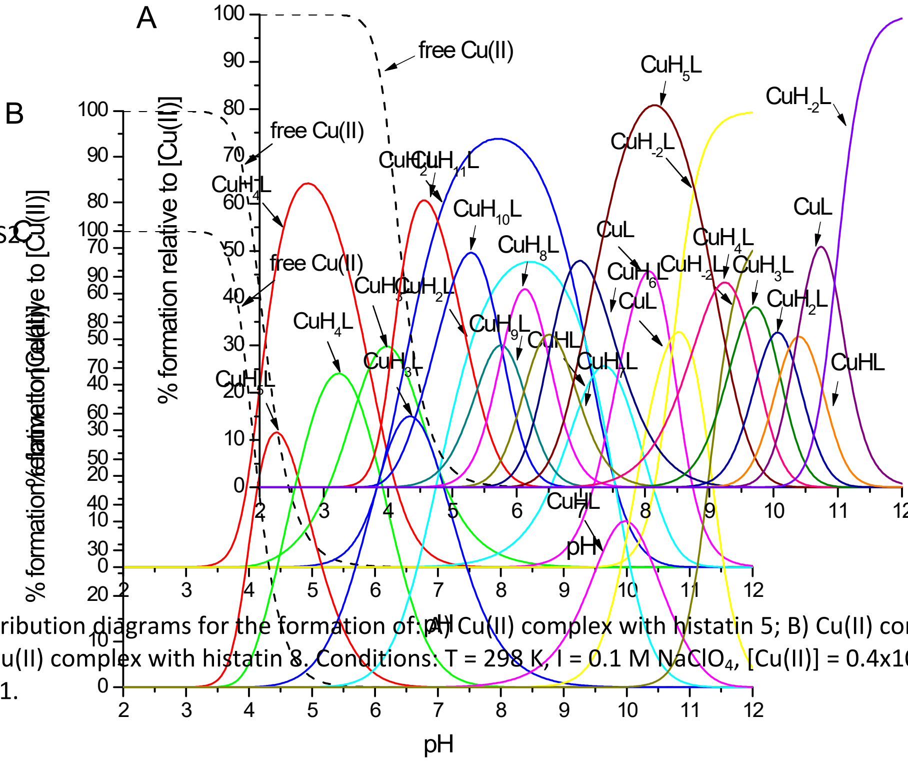

Fig S2

Distribution diagrams for the formation of: A) Cu(II) complex with histatin 5; B) Cu(II) complex with histatin 5-8; C) Cu(II) complex with histatin 8. Conditions: T = 298 K, I = 0.1 M $NaClO_4$, [Cu(II)] = $0.4x10^{-3}$ M; M:L molar ratio = 0.8:1.

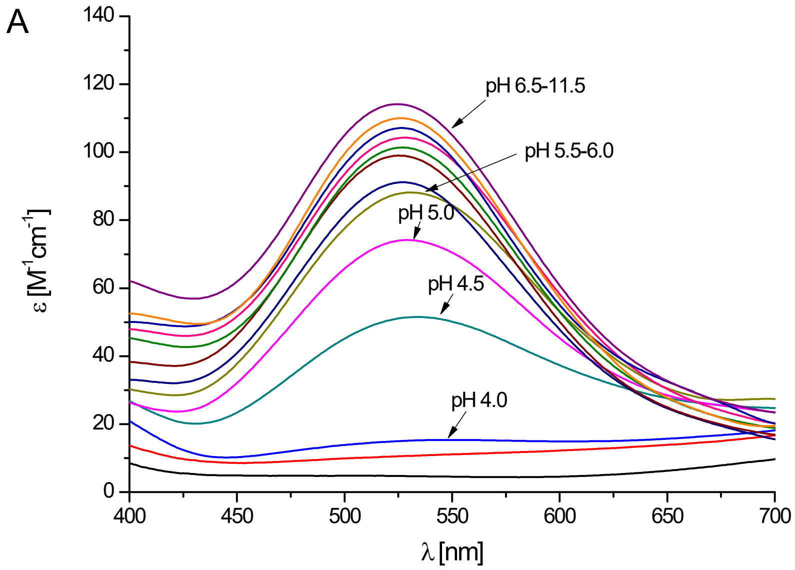

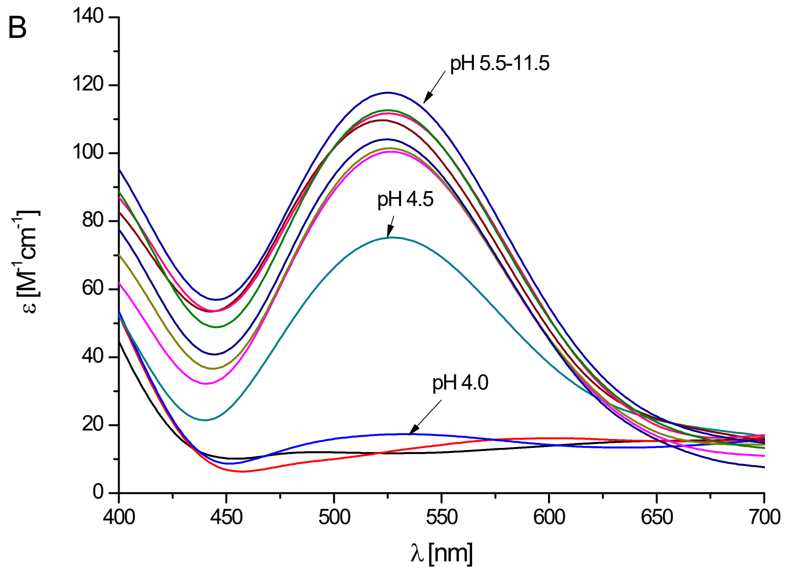

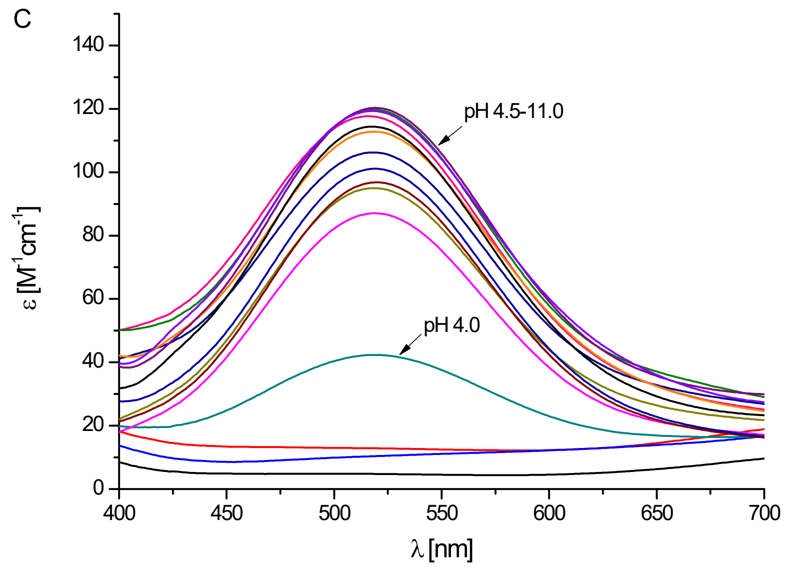

Fig. S3. UV-Vis spectra of Cu(II) complexes with: A) histatin 5; B) histatin 5-8; C) histatin 8; in pH range 2-11. Conditions: T = 298 K, I = 0.1 M $NaClO_4$, [Cu(II)] = $0.4.10^{-3}$ M; M:L molar ratio = 0.8:1.

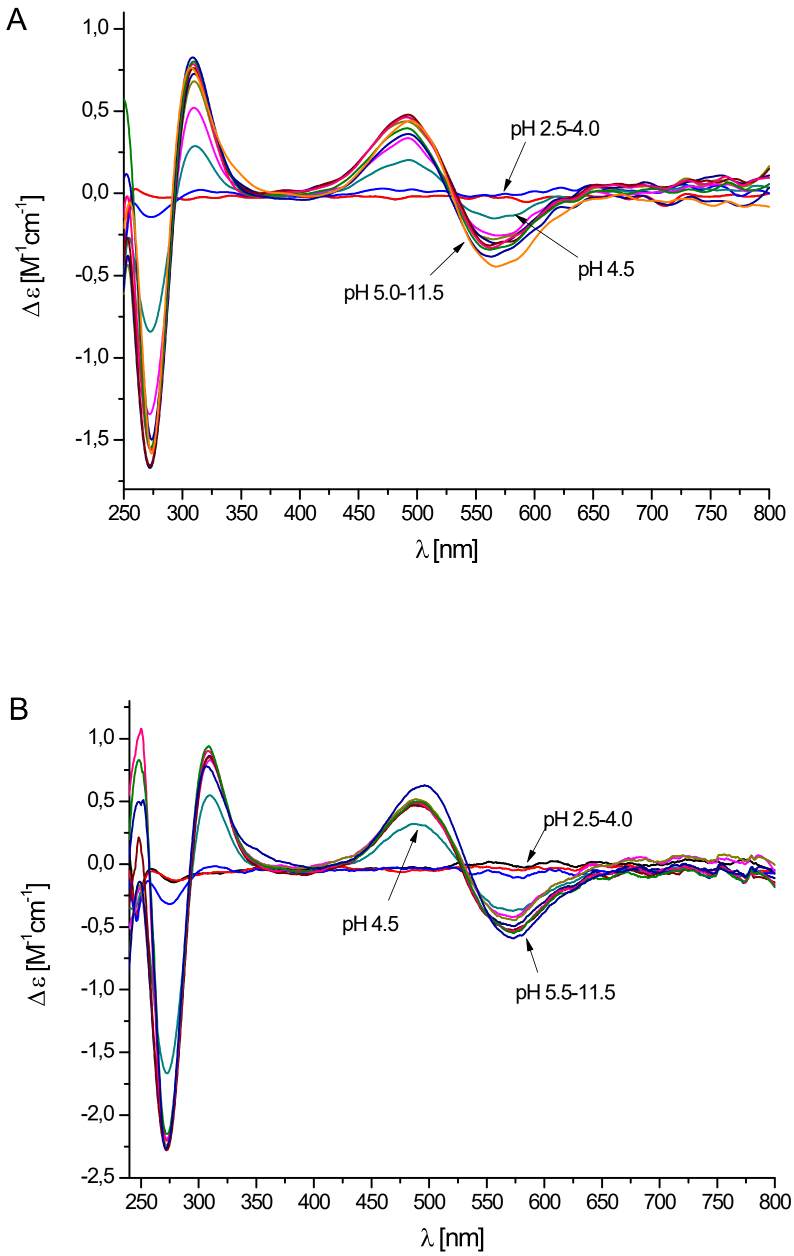
A
1,0
0,5
0,0
-0,5
-1,0
-1,5
Δε [M-1cm-1]
250 300 350 400 450 500 550 600 650 700 750 800
λ [nm]
pH 2.5-4.0
pH 4.5
pH 5.0-11.5
B
1,0
0,5
0,0
-0,5
-1,0
-1,5
-2,0
-2,5
Δε [M-1cm-1]
250 300 350 400 450 500 550 600 650 700 750 800
λ [nm]
pH 2.5-4.0
pH 4.5
pH 5.5-11.5

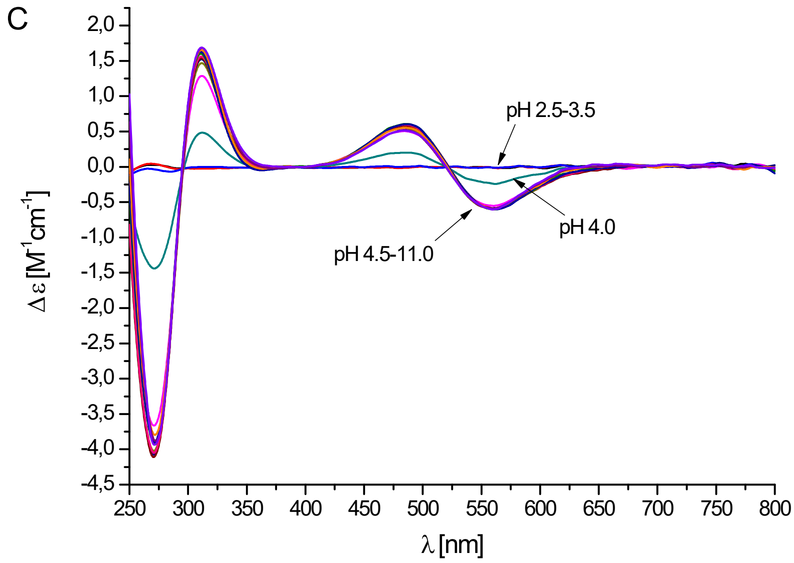

Fig. S4. CD spectra of Cu(II) complexes with: A) histatin 5; B) histatin 5-8; C) histatin 8; in pH range 2-11. Conditions: T = 298 K, I = 0.1 M $NaClO_4$, [Cu(II)] = $0.4.10^{-3}$ M; M:L molar ratio = 0.8:1.

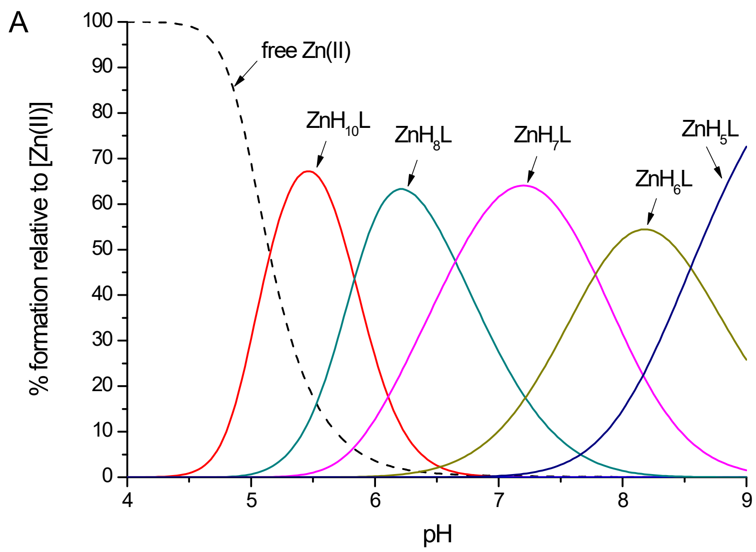

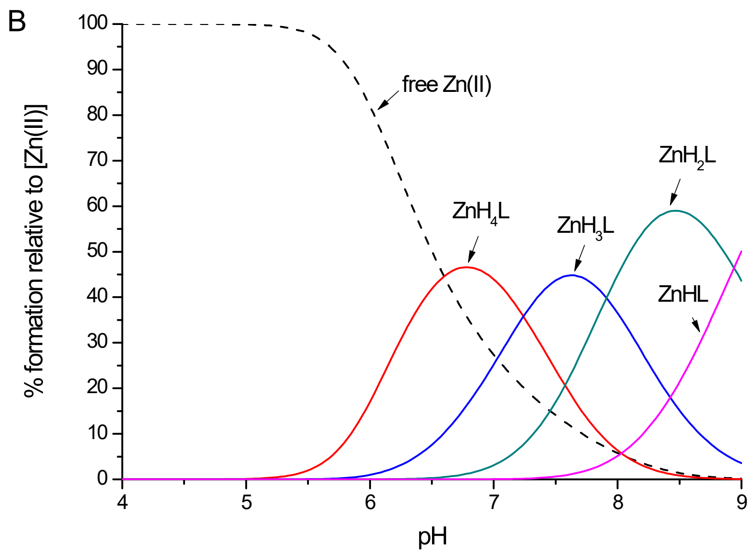

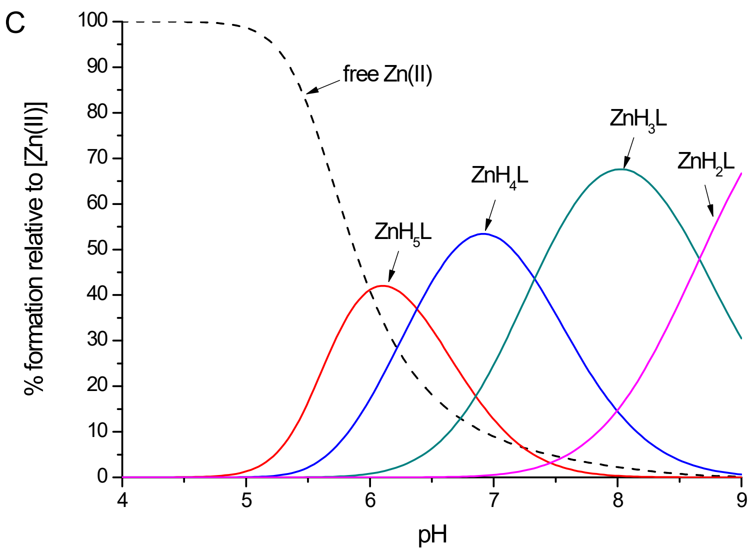

Fig. S5. Distribution diagrams for the formation of: A) Zn(II) complex with histatin 5; B) Zn(II) complex with histatin 5-8; C) Zn(II) complex with histatin 8. Conditions: T = 298 K, I = 0.1 M $NaClO_4$, [Zn(II)] = 0.4×10^{-3} M; M:L molar ratio = 0.8:1.

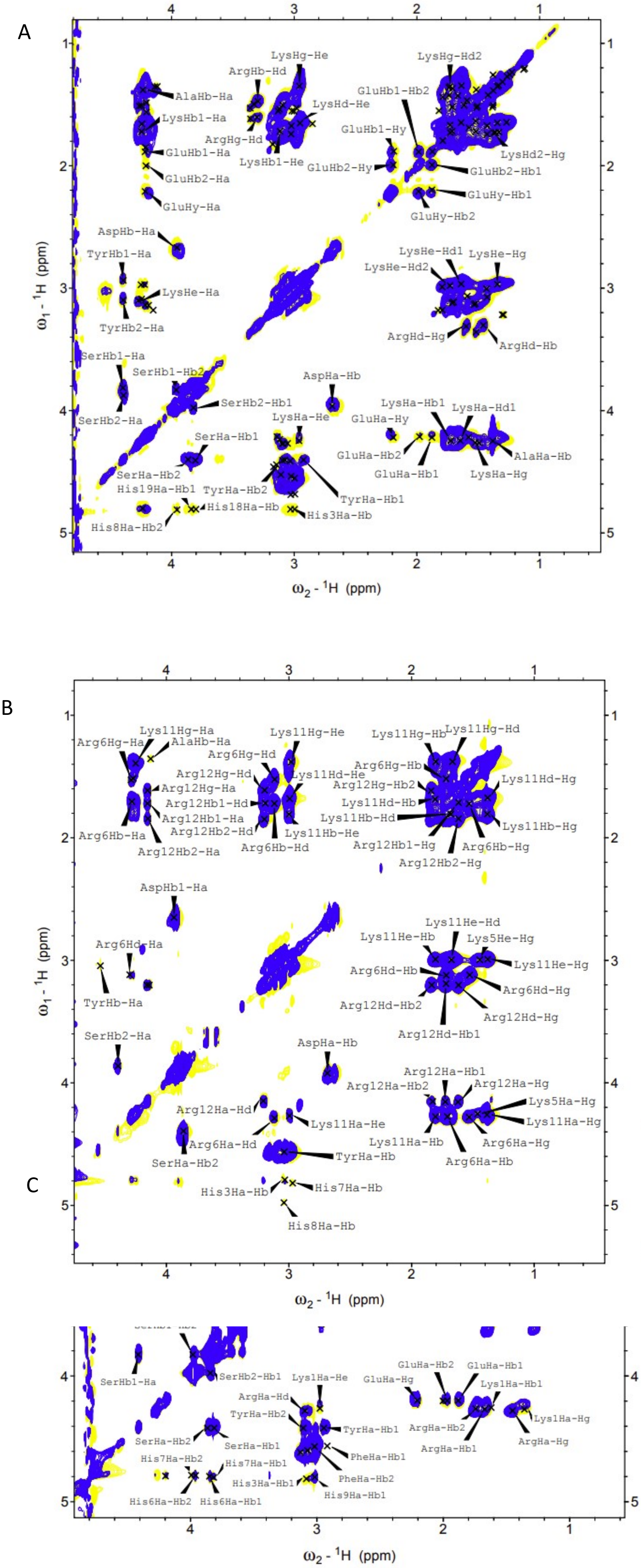
A
AlaHb-Ha
LysHb1-Ha
GluHb1-Ha
GluHb2-Ha
GluHy-Ha
ArgHb-Hd
ArgHg-Hd
LysHg-He
LysHd-He
LysHb1-He
LysHg-Hd2
GluHb1-Hb2
GluHb1-Hy
GluHb2-Hy
GluHb2-Hb1
GluHy-Hb1
GluHy-Hb2
LysHd2-Hg
AspHb-Ha
TyrHb1-Ha
TyrHb2-Ha
LysHe-Ha
LysHe-Hd1
LysHe-Hd2
LysHe-Hg
ArgHd-Hg
ArgHd-Hb
SerHb1-Ha
SerHb1-Hb2
SerHb2-Hb1
SerHb2-Ha
AspHa-Hb
SerHa-Hb1
LysHa-He
LysHa-Hb1
LysHa-Hd1
GluHa-Hy
GluHa-Hb2
GluHa-Hb1
LysHa-Hg
AlaHa-Hb
SerHa-Hb2
His19Ha-Hb1
TyrHa-Hb2
TyrHa-Hb1
His18Ha-Hb
His3Ha-Hb
His8Ha-Hb2
ω1 - 1H (ppm)
ω2 - 1H (ppm)
B
Lys11Hg-Ha
AlaHb-Ha
Arg6Hg-Ha
Arg12Hg-Ha
Arg12Hb1-Ha
Arg6Hb-Ha
Arg12Hb2-Ha
Lys11Hg-He
Arg6Hg-Hd
Arg12Hg-Hd
Lys11Hd-He
Arg12Hb1-Hd
Arg12Hb2-Hd
Lys11Hb-He
Arg6Hb-Hd
Lys11Hg-Hb
Lys11Hg-Hd
Arg6Hg-Hb
Arg12Hg-Hb2
Lys11Hd-Hb
Lys11Hb-Hd
Lys11Hd-Hg
Lys11Hb-Hg
Arg12Hb1-Hg
Arg6Hb-Hg
Arg12Hb2-Hg
AspHb1-Ha
Arg6Hd-Ha
TyrHb-Ha
Lys11He-Hd
Lys11He-Hb
Lys5He-Hg
Lys11He-Hg
Arg6Hd-Hb
Arg6Hd-Hg
Arg12Hd-Hb2
Arg12Hd-Hg
Arg12Hd-Hb1
SerHb2-Ha
AspHa-Hb
Arg12Ha-Hb1
Arg12Ha-Hb2
Arg12Ha-Hg
Lys5Ha-Hg
Lys11Ha-Hg
Arg12Ha-Hd
Lys11Ha-He
Arg6Ha-Hd
Lys11Ha-Hb
Arg6Ha-Hg
SerHa-Hb2
TyrHa-Hb
Arg6Ha-Hb
His3Ha-Hb
His7Ha-Hb
His8Ha-Hb
ω1 - 1H (ppm)
ω2 - 1H (ppm)
C
SerHb1-Ha
SerHb2-Hb1
Lys1Ha-He
GluHa-Hg
GluHa-Hb2
GluHa-Hb1
Lys1Ha-Hb1
ArgHa-Hd
TyrHa-Hb2
TyrHa-Hb1
Lys1Ha-Hg
ArgHa-Hb2
ArgHa-Hb1
ArgHa-Hg
SerHa-Hb2
SerHa-Hb1
PheHa-Hb1
PheHa-Hb2
His7Ha-Hb2
His7Ha-Hb1
His3Ha-Hb1
His9Ha-Hb1
His6Ha-Hb2
His6Ha-Hb1
ω2 - 1H (ppm)

Fig S6. ^{1}H–^{1}H TOCSY NMR spectra of a fragment of the ligand (yellow) and the Zn(II) complex (blue) with the (A) histatin 5, (B) histatin 5-8 and (C) histatin 8. Conditions: [histatin 5] = [histatin 5-8] = [histatin 8] = 1 mM, [Zn(II)] = 1 mM, pH = 7.4, T = 298 K.

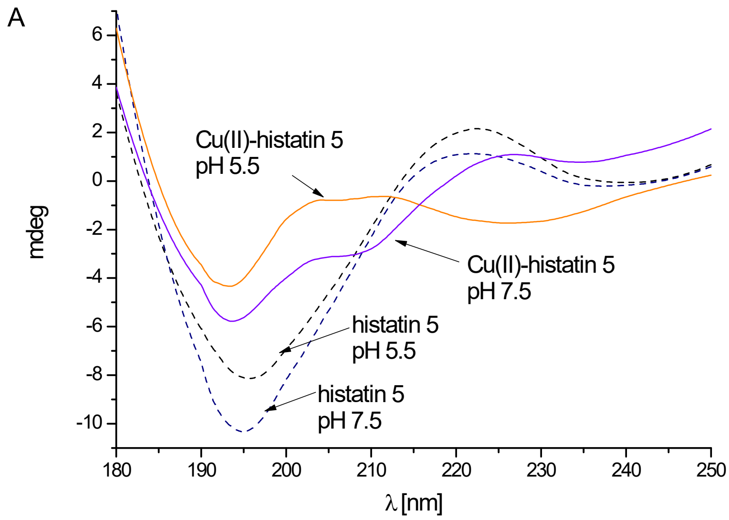

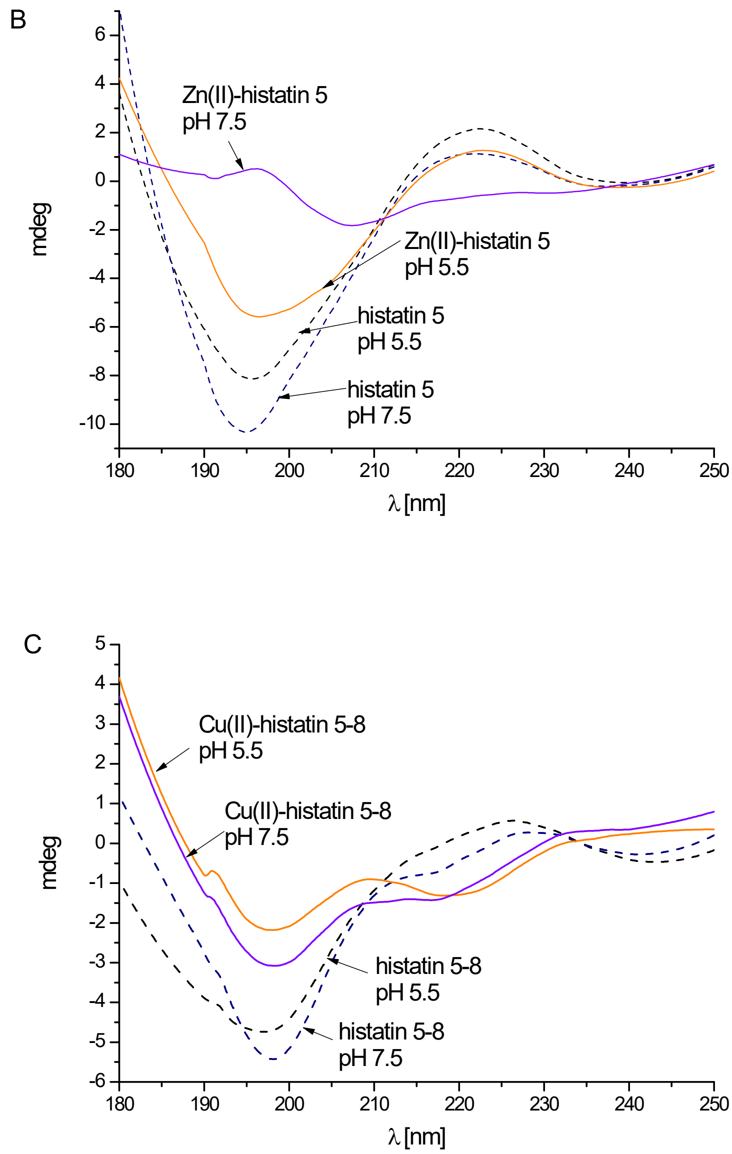
B
C
Zn(II)-histatin 5
pH 7.5
Zn(II)-histatin 5
pH 5.5
histatin 5
pH 5.5
histatin 5
pH 7.5
Cu(II)-histatin 5-8
pH 5.5
Cu(II)-histatin 5-8
pH 7.5
histatin 5-8
pH 5.5
histatin 5-8
pH 7.5
mdeg
λ [nm]

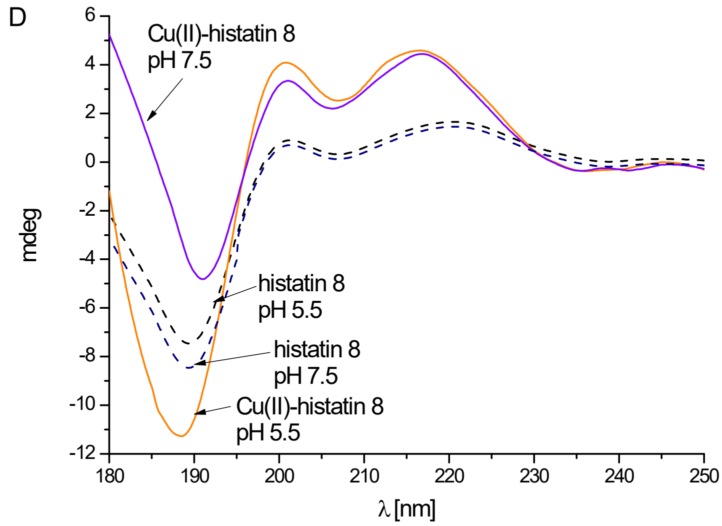

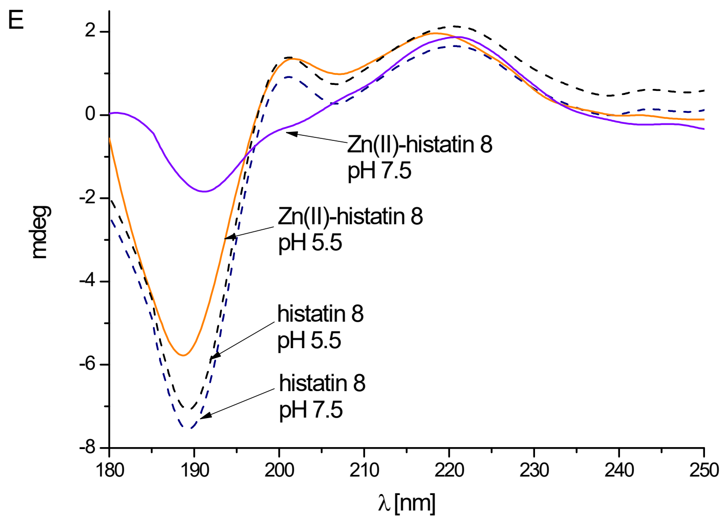

Fig. S7. Comparison of CD spectra of (A) histatin 5 and its Cu(II) complex, (B) histatin 5 and its Zn(II) complex, (C) histatin 5-8 and its Cu(II) complex, (D) histatin 8 and its Cu(II) complex and (E) histatin 8 and its Zn(II) complex at pH 5.5 and 7.5. Conditions: T = 298 K, I = 0.1 M $NaClO_4$, [Cu(II)] = [Zn(II)] = $0.4.10^{-3}$ M; M:L molar ratio = 0.8:1, optical path = 0.01 cm.

Table S2. Examples of MIC breakpoints values from EUCAST/2024/01/21 for bacteria.[1]

Enterococcus ssp. (for *E. faecalis*)	MIC breakpoints (µg/mL)		Staphylococcus spp. (for *S. aureus*)	MIC breakpoints (µg/mL)	
	S≤	R>		S≤	R>
Ampicillin	4	8	Azithromycin	2	2
Ampicillin-Sulbactam	4	8	Ceftobiprole	2	2
Amoxicillin	4	8	Ciprofloxacin	0.001	2
Amoxicillin-clavulanic acid	4	8	Daptomycin	1	1
Imipenem	0.001	4	Moxifloxacin	0.25	0.25

Ciprofloxacin	4	4	Amikacin	16	16
Levofloxacin	4	4	Gentamicin	2	2
Vancomycin	4	4	Tobramycin	2	2
Linezolid	4	4	Teicoplanin	2	2
Nitrofurantoin	64	64	Clindamycin	0.25	0.25

References:

1 The European Committee on Antimicrobial Susceptibility Testing. Breakpoint tables for interpretation of MICs and zone diameters. Version 14.0, 2024. http://www.eucast.org.